6. References

1. Aoki H. Science and medical application of hydroxyapatite. Takayama Press System Center Co., Inc., 1991.
2. Suchanek W, Yashima M, Kakihana M, Yoshimura M. Hydroxyapatite/hydroxyapatite-whisker composites without sintering additives: mechanical properties and microstructural evolution. J Am Ceram Soc 1997;80:2805-2813.
3. Kothaplli CR, Wei M, Legeros RZ, Shaw MT. Influence of temperature and aging time on HA synthesized by the hydrothermal method. J Mater Sci: Mater Med 2005;16:441-446
4. Furuzono T, Sonoda K, Tanaka J. A hydroxyapatite coating covalently linked onto a silicone implant material. J Biomed Mater Res 2001;56:9-12.
5. Furuzono T, Kishida A, Tanaka J. Nano-scaled hydroxyapatite/polymer composite I. Coating of sintered hydroxyapatite particles on poly(γ-methacryloxypropyl trimethoxysilane)-grafted silk fibroin fibers through chemical bonding. J Mater Sci: Mater Med 2004;15:19-23.
6. Furuzono T, Wang P, Korematsu A, Miyazaki K, Oido-Mori M, Kowashi Y, Ohura K, Tanaka J, Kishida A. Physical and biological evaluations of sintered hydroxyapatite/silicone composite with covalent bonding for a percutaneous implant material. J Biomed Mater Res B: Appl Biomater 2003;65B:217-226.
7. Jarcho M, Bolen CH, Thomas MB, Bobick J, Kay JF, Doremus RH. Hydroxylapatite synthesis and characterization in dense polycrystalline form. J Mater Sci 1976;11:2027-2035.
8. Schmidt HK. Nanoparticles for ceramic and nanocomposite processing. Mol Cryst Liq Cryst 2000;353:165-179.
9. Cushing BL, Kolesnichenko VL, O'Connor CJ. Recent advances in the liquid-phase syntheses of inorganic nanoparticles. Chem Rev 2004;104:3893-3946.
10. Masuda Y, Matsubara K, Sakka S. Synthesis of hydroxyapatite from metal alkoxides

through sol-gel technique. J Ceram Sci Japan 1990;98:1226-1277.

11. Sanchez C, Livage J. Sol-gel chemistry from metal alkoxide precursors. New J Chem 1990;14:513-521.

12. Schmidt HK, Geiter E, Mennig M, Krug H, Becker C, Winkler R-P. The sol-gel process for nano-technologies: new nanocomposites with interesting optical and mechanical properties. J Sol-Gel Sci Tech 1998;13:397-404.

13. Lim GK, Wang J, Ng SC, Gan LM. Processing of fine hydroxyapatite powders via an inverse microemulsion route. Mater Lett 1996;28:431-436.

14. Sonoda K, Furuzono T, Walsh D, Sato K, Tanaka J. Influence of emulsion on crystal growth of hydroxyapatite. Solid State Ionics 2002;151:321-327.

15. Kawasaki T. Hydroxyapatite as a liquid chromatographic packing. J Chromatogr 1991;544:147-184.

16. Frenkel J. Viscous flow of crystalline-bodies under the action of surface tension. J Phys USSR 1945;9:385-391

17. Kuczynski GC. Self-Diffusion in Sintering of Metallic Particles. Trans AIME 1949;185:169-178.

18. Barralet JE, Best SM, Bonfield W. Effect of sintering parameters on the density and microstructure of carbonate hydroxyapatite. J Mater Sci: Mater Med 2000;11:719-724.

19. Landi E, Tampieri A, Celotti G, Sprio S. Densification behaviour and mechanisms of synthetic hydroxyapatites. J Eur Ceram Soc 2000;20:2377-2387.

20. Bernache-Assollant D, Ababoua A, Championa E, Heughebaertb M. Sintering of calcium phosphate hydroxyapatite $Ca_{10}(PO_4)_6(OH)_2$ I. Calcination and particle growth. J Eur Ceram Soc 2003;23:229-241.

21. Somiya S, Ioku K, Yoshimura M. Hydrothermal synthesis and characterization of fine

apatite crystals. Mater Sci Forum 1988;34-36:371-378.

22. Yoshimura M, Suda H, Okamoto K, Ioku K. Hydrothermal synthesis of biocompatible whiskers. J Mater Sci 1994;29:3399-3402.

23. Papargyris AD, Botis AI, Papargyri SA. Synthetic routes for hydroxyapatite powder production. Key Eng Mater 2002;206-213:83-86

24. Carless JE, Foster AA. Accelerated crystal growth of sulfathiazole by temperature cycling. J Pharmaceut Pharmacol 1966;18:697-708.

25. Wei M, Ruys AJ, Milthorpe BK, Sorrell CC. Solution ripening of hydroxyapatite nanoparticles: effects on electrophoretic deposition. J Biomed Mater Res 1999;45:11-19.

26. Okada M, Furuzono T. Fabrication of high-dispersibility nanocrystals of calcined hydroxyapatite. J Mater Sci in contribution

27. Sindhu S, Valiyaveettil S. Design and synthesis of optically transparent calcium incorporated polymer complex. J Polym Sci B: Polym Phys 2004;42:4459-4465

28. Misra DN. Adsorption of low-molecular-weight sodium polyacrylate on hydroxyapatite. J Dent Res 1993;10:1418-1422.

29. Yoshida Y, Van Meerbeek B, Nakayama Y, Yoshioka M, Snauwaert J, Abe Y, Lambrechts P, Vanherle G, Okazaki M. Adhesion to and decalcification of hydroxyapatite by carboxylic acids. J Dent Res 2001;80:1565-1569.

30. Bonapasta AA, Buda F, Colombet P. Interaction between Ca Ions and Poly(acrylic acid) Chains in Macro-Defect-Free Cements: A Theoretical Study. Chem Mater 2001;13:64-70.

31. Emerson WH, Fisher EE. The infrared absorption spectra of carbonate in calcified tissue. Arch Oral Biol 1962;7:671-683.

32. Bonel G, Heughebaert J-C, Heughebaert M, Lacout JL, Lebugle A. Apatitic calcium orthophosphates and related compounds for biomaterials preparation. Ann NY Acad Sci

1988;523:115-130.

33. Suetsugu Y, Hirota K, Fujii K, Tanaka J. Compositional distribution of hydroxyapatite surface and interface observed by electron spectroscopy. J Mater Sci 1996;31:4541-4544.

34. Gibson IR, Bonfield W. Novel synthesis and characterization of an AB-type carbonate-substituted hydroxyapatite. J Biomed Mater Res 2002;59:697-708.

35. Furuzono T, Masuda M, Okada M, Yasuda S, Kadono H, Tanaka R, Miyatake K. Increase of cell adhesiveness on poly(ethylene terephthalate) fabric by coating of sintered hydroxyapatite nanocrystals for development of an artificial blood vessel. ASAIO J in contribution

Figure captions

Fig. 1 Schematic model for the fabrication of single nanocrystals of hydroxyapatite calcined with an anti-sintering agent and subsequently removing the agent

Fig. 2 FT-IR spectra of (a) poly(acrylic acid) (PAA); (b) poly(acrylic acid calcium salt) (PAA-Ca) precipitated by adding a saturated $Ca(OH)_2$ *aq.* in a PAA aqueous solution ($PAA/Ca(OH)_2$ = 1/1 w/w); (c) PAA-Ca after calcination at 800°C for 1 h at a heating rate of 10°C/min

Fig. 3 Thermal decomposition behavior of (a) $CaCO_3$ with calcite structure and (b) PAA-Ca at a heating rate of 10°C/min in air

Fig. 4 XRD patterns of HAp nanocrystals calcinated (a) without additive and (b) with PAA-Ca at 800°C for 1 h at a heating rate of 10°C/min in air

Fig. 5 FT-IR spectra of (a) a mixture of HAp particles and PAA-Ca prepared by addition of saturated $Ca(OH)_2$ *aq.* in PAA-stabilized HAp aqueous dispersion, (b) the HAp/PAA-Ca mixture after calcination at 800°C for 1 h, (c) HAp nanocrystals after washing with water, and (d) HAp crystals after calcination without additives

Fig. 6 SEM photographs of (a) original HAp particles before calcination, and HAp crystals after calcination (b) without additive and (c) with PAA-Ca. (d) A TEM photograph and (e) the associated electron diffraction pattern of a HAp crystal calcined with PAA-Ca, showing the crystal consisting of a single HAp phase.

Fig. 7 Size distributions of (a) original HAp particles before calcination, and HAp crystals after calcination (b) without additive and (c) with PAA-Ca. The size distributions were measured in ethanol.

Fig. 8 Specific surface areas of (a) original HAp particles, and HAp crystals after calcination (b) without additive and (c) with PAA-Ca. Error bars represent standard deviations of triplicates (** $p < 0.01$).

Table 1 Ca/P molar ratio of HAp after calcination at 800°C for 1 h at a heating rate of 10°C/min

	Ca/P (molar ratio)	
	ICP[a)]	XPS[b)]
Without additive	1.67	1.51
With PAA-Ca	1.72	1.64

[a)] Measured by inductively coupled plasma-atomic emission spectrometry
[b)] X-ray photoelectron spectroscopy

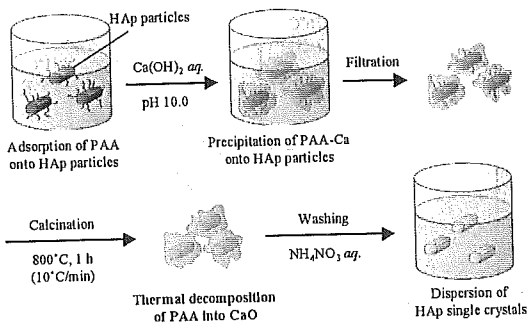

Fig. 1 Okada *et al*

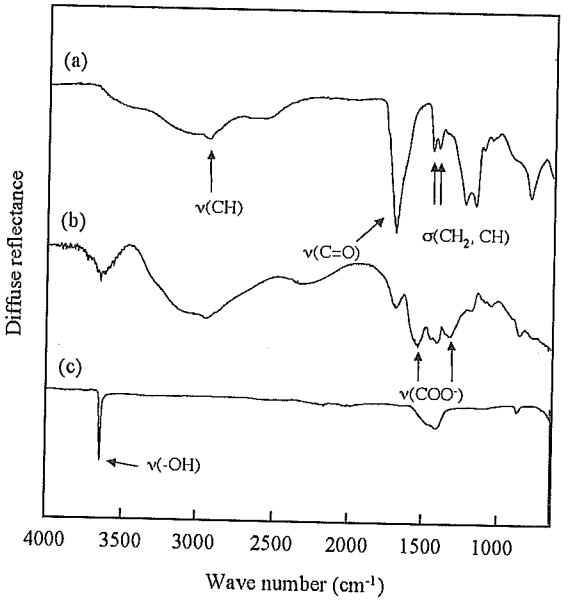

Fig. 2 Okada *et al*

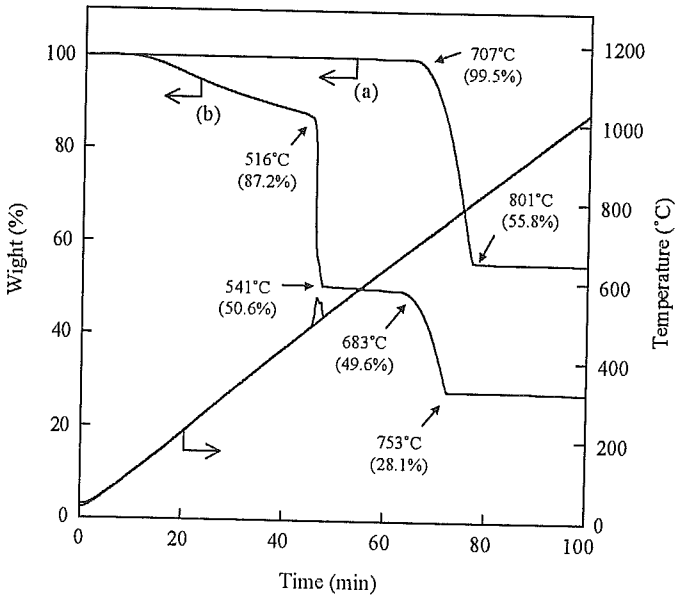

Fig. 3 Okada *et al*

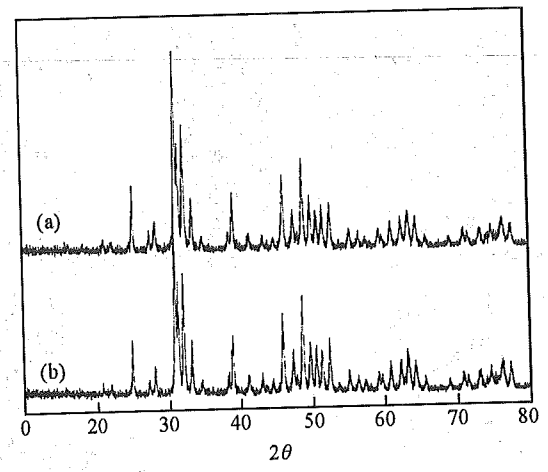

Fig. 4 Okada *et al*

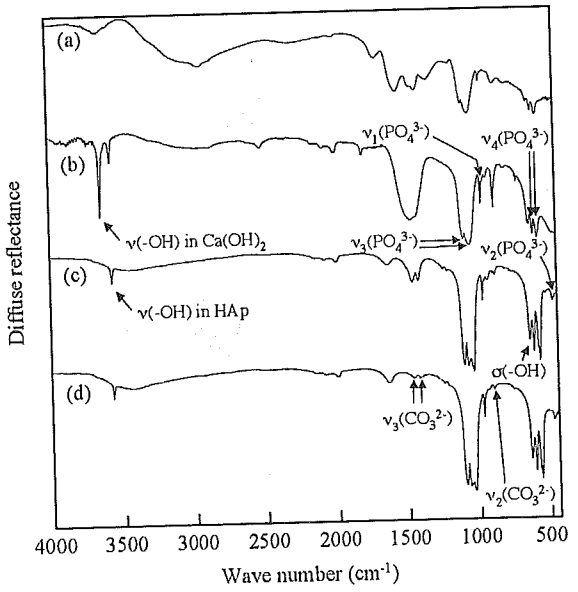

Fig. 5 Okada *et al*

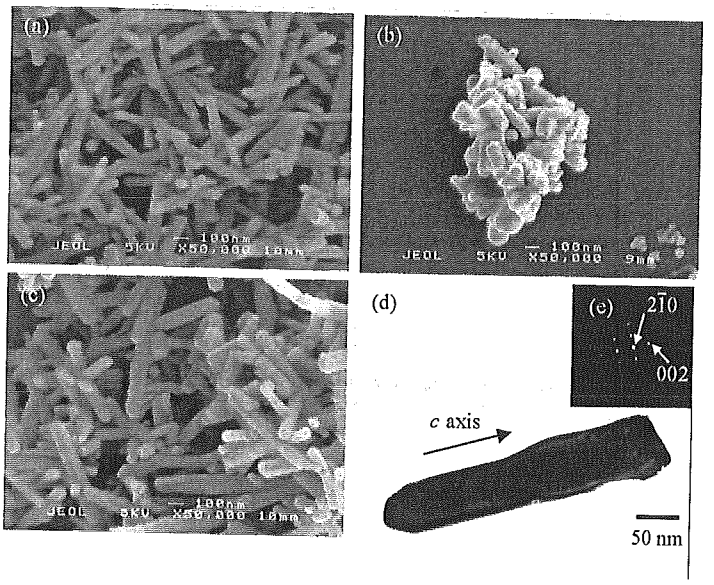

Fig. 6 Okada *et al*

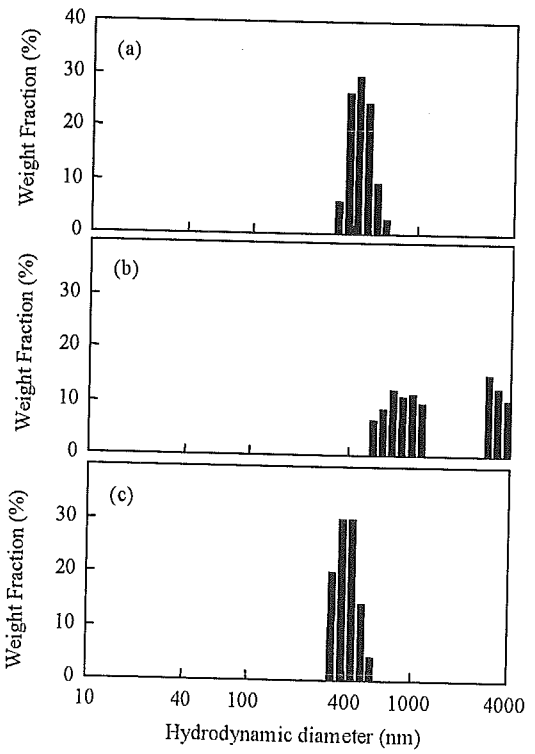

Fig. 7 Okada *et al*

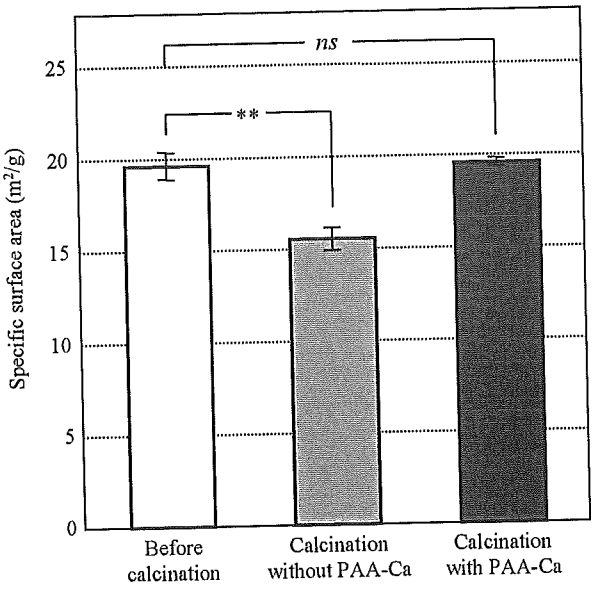

Fig. 8 Okada *et al*

Fabrication of calcined hydroxyapatite nanocrystals-coated stainless steel and morphological influence of nanocrystals on cell activity

Masahiro Okada[1], Miwa Masuda[1], Ryoichi Tanaka[2], Kunio Miyatake[3], Daisuke Kuroda[4], Tsutomu Furuzono[1,*]

[1]Department of Bioengineering, National Cardiovascular Center Research Institute, 5-7-1 Fujishirodai, Suita, Osaka 565-8565, Japan

[2]Department of Radiology, National Cardiovascular Center, 5-7-1 Fujishirodai, Suita, Osaka 565-8565, Japan

[3]National Hospital Organization Osaka Minami Medical Center, 2-1 Kido-higashimachi, Kawachinagano, Osaka 586-8521, Japan

[4]Reconstitution Materials Group, Biomaterials Center, National Institute for Materials Science, 1-1 Namiki, Tsukuba, Ibaraki 305-0044, Japan

*Author to whom all correspondence should be addressed:

Tel: +81-6-6833-5012 (ext 2623)

Fax: +81-6-6872-7485

E-mail: furuzono@ri.ncvc.go.jp

Abstract

Nano-sized single crystals of hydroxyapatite (HAp) having spherical or rod-like morphologies were coated through covalently linkage onto a Type 316L stainless-steel substrate, which was chemically modified by graft polymerization of γ-methacryloxypropyl triethoxysilane (MPTS). The grafting of poly(MPTS) on the substrate was confirmed by X-ray photoelectron spectroscopy and attenuated total reflection Fourier transform infrared spectroscopy. In order to coat the substrate with the HAp crystals through covalent linkage, the reaction between alkoxysilyl groups in the poly(MPTS) grafted on the substrate and OH groups on the HAp crystals was conducted at 80°C. The poly(MPTS)-grafted substrate was uniformly and strongly coated by the HAp nanocrystals, although the HAp crystals adsorbed physically on the original substrate without poly(MPTS) grafting were almost removed by ultrasonic treatment. Human umbilical vein endothelial cells (HUVEC) adhered more plentifully on the HAp-coated stainless-steel substrate as compared to original substrate after only 4 h of initial incubation. The amount of HUVEC adhesion and proliferation on the rod-like HAp-coated substrate was larger than the spherical one at the same coverage ratio by HAp crystals, which seems to be due to a larger cationic charge. (The amount of HUVEC adhesion on the HAp-coated substrate increased with an increase in the surface-coverage ratio by the HAp crystals, and showed plateau over ??% coverage by the HAp crystals.)

(183 words)

1. Introduction

Hydroxyapatite (HAp), a kind of bioceramics, has been extensively used as implant materials for orthopaedic and dental applications, because it bonds directly to bone when implanted [1-5], resulting in the formation of a strong bone-implant interface. Recently, HAp ceramics has also attracted attention as a soft-tissue compatible material through the development of percutaneous devices [6]. However, owing to its mechanical weakness and brittleness, applications of HAp have been confined to those with low mechanical stress

We have recently developed a novel inorganic/organic nanocomposite for a soft-tissue-compatible material [7-9]: a silk fibroin or a poly(ethylene terephthalate) fiber, whose surface was modified with calcined HAp crystals through covalent linkage. The novel composite almost retained the flexibility of the polymer substrate and showed good tissue adhesion due to the HAp crystals on the surface [10]. The coating of sintered HAp nanocrystals was an effective way to give tissue-adhesion activity to substrates without a coating of adhesion proteins derived from animals, such as collagen and gelatin, which are feared due to the possible outbreak of infectious diseases such as bovine spongiform encephalopathy (BSE).

If our HAp nanocrystal coating technique can be applied to other biomaterials as well as polymer compounds, the uses are expected to spread widely in medical fields. In this regard, a metal substrate, Type 316L stainless-steel, was selected in this study. Stainless steel is one of the most important biomedical metal compounds in medical fields, and has been used as artificial bones [11] or stents [12] and so on. The surface modification of metallic compounds with HAp has been studied to improve surface properties of metallic compounds: plasma-sprayed coating [13] sputtering coating [14-16], treatment with simulated body fluid [17], electrophoretic deposition [18, 19]. The HAp obtained by the above methods had amorphous structure or low

crystallinity, and the interaction at the interface between HAp and the metal surface was weak [13]. Accordingly, the heat treatment around 1000°C is needed to crystallize HAp and to obtain more strong interaction between HAp and the metal surface [20]. There is, however, concern about the effects of the high temperature treatment on the metallic compounds and the HAp coating layer: precipitation of carbide ($Cr_{23}C_6$) and intermetallic phases at grain boundaries by heat treatment of Type 316 austenitic stainless steel at 500-900°C [21]; metal-catalysed degradation and shringage-induced cracking of the HAp layer [22]

The present study overcome the above problems by utilizing our novel coating method for Type 316L stainless-steel substrate with calcined HAp nanocrystals through covalent linkage, which are shown in Fig, 1. Donation of covalent boding between HAp nanocrystals and the substrate was carried out at 80°C by a coupling reaction between hydroxyl groups in the HAp crystal and alkoxysilyl groups of the polymer grafted on the substrate. The influences of the morphology of HAp and the surface coverage ratio by HAp was evaluated by cell adhesion tests.

Materials and methods

Materials

The Type 316L stainless steel used in this study had a disk shape with 12-mm diameter and 3-mm height, and the following bulk composition: C, 0.02%; Ni, 12.12%; Cr, 17.2%; Si, 0.48%; Mn, 1.39%; P, 0.33%; S, 0.24%; Fe, balance. The silane coupling agent, 3-mercaptopropyltrimethoxysilane, of 95% purity was obtained from Sigma-Aldrich Co., WI, USA. γ-Methacryloxypropyl trimethoxysilane (MPTS) used as monomer was donated by Shin-Etsu Chemical Industries Co., Tokyo, Japan.. 2,2'-azobis(isobutyronitrile) (AIBN; Nacalai

Tesque Inc., Kyoto, Japan) used as radical initiator was purified by recrystallization. Water was purified with a Milli-Q system (Millipore Corp., Bedford, Mass.). Other materials were reagent grade and purchased from Nacalai Tesque Inc.

HAp crystals with spherical or rod-like morphology were prepared by a modified emulsion system [23]. The HAp crystals were used after calcination at 800°C for 1 h with an anti-sintering agent surrounding the HAp crystals to prevent the calcination-induced sintering among the crystals [24-25]. The agent was removed by washing with water, and then the HAp crystals were dispersed in ethanol medium.

Silanization of the stainless-steel substrate

First, the stainless-steel substrates were cleaned ultrasonically in an acetone bath for 30 min. After that, the substrate were chemically treated in a concentrated nitric acid aqueous solution for 30 min, rinsed thoroughly with water, and blown dry with nitrogen. The silanization of the substrate was performed at room temperature in 10 mM ethanol solution of silane coupling agent for 3 h. The silanized substrate was rinsed with ethanol and water to remove unreacted agents. It was then blown gently with nitrogen and aged at 110°C for 1 h.

Graft-polymerization of MPTS onto silanized stainless-steel substrate

Graft polymerization of MPTS onto the silanized stainless-steel substrate was conducted according to a literature [25] as follows. The substrate was carefully immersed in a 100-mL flask equipped with an inlet of N_2, a reflux condenser, and a stirrer, and then purged with N_2 for 30min. 25 mL of anhydrous toluene was added in the flask. After the temperature of the mixture was raised to 70°C, and 3.3 mL of MPTS monomer and 5 ml of anhydrous toluene solution containing 33 mg of AIBN was respectively added, and stirred occasionally during polymerization at 70°C

for 2 h. After the polymerization, the substrate was washed with ethanol several times to remove homopolymers formed during polymerization, and then dried under reduced pressure for 1 h at 70°C.

Coating of HAp nanocrystals on PET

The poly(MPTS)-grafted stainless-steel substrate was soaked in the HAp suspension (2.0 wt/v%) in ethanol for 1 h at room temperature to adsorb the crystals on the grafted substrate, washed with ethanol, and then heated at 80°C for 2 h under vacuum (1 mmHg) in order to form covalent bonding by the reaction between OH groups on the HAp crystals with alkoxysilyl groups on the poly(MPTS) grafted on the substrate. The composite was washed in ethanol with an ultra sonic generator (output: 20 kHz and 35W) for 2 min to remove unreacted HAp crystals, which were physically adsorbed on other crystals. The composite was finally washed in a large amount of ethanol and water to remove the residual organic compounds.

Cell adhesiveness

Human umbilical vein endothelial cells (HUVEC) were placed onto the HAp-coated stainless steel composite in 24-well multiplates at 1 x 10^5 cells/well in a Endothelial cell basal medium-2 (EGM-2, supplemented with heat-inactivated 5% fetal bovine serum (FBS,) 1 mg/ml of gentamicin/amphoterisin B), and incubated at 37 °C for 4 h. For scanning electron microscope (SEM) observation, they were washed twice in phosphate-buffered saline [PBS(-)], the cells were fixed with 10% buffered glutaraldehyde for 20 min at room temperature, and then rinsed with PBS(-) three times. The cells were dehydrated with aqueous ethanol (50-100%) and 100% *n*-butanol for 5 min at room temperature step by step. The samples were lyophilized and coated with gold.

Measurements

The stainless steel substrates and the cell morphologies were observed with a 5 kV scanning electron microscope (SEM; JSM-6301F, JEOL, Tokyo, Japan). The surface-modification of the substrate was confirmed by attenuated total reflection Fourier transform infrared spectroscopy (ATR FT-IR; Spectrum One, Perkin-Elmer Inc., MA) at 4-cm^{-1} resolution with 16 scans, and X-ray photoelectron spectroscopy (XPS; PHI Model 1600S, Physical Electronics, Inc. MN) with 100-W non-monochromated MgK source at an emission angle of 45° and an investigated size of 0.8 x 2.0 mm.

Results and Discussion

The procedure for the coating of stainless-steel substrate with nano-sized HAp crystals is sketched in Fig. 1. In order to covalently link with the substrate and the HAp crystals, first, the substrate was chemically modified with poly(MPTS), in which alkoxysilyl groups can be coupled with OH groups on HAp surfaces [26]. Although the physical adsorption of the homopolymer of MPTS directly onto a substrate is the simplest method for the modification, it was not the most reliable way to obtain a poly(MPTS)-modified surface as discussed below. Accordingly, the graft polymerization was coducted in this study to link covalently between poly(MPTS) and the substrate, that is, to prepare the permanently modified surface. Before the graft polymerization, the modification with 3-mercaptopropyltrimethoxysilane having mercapto groups was conducted. Mercapto group was selected because it has large transfer coefficient for radicals [26]

Table 1 shows the surface composition of the original, silanized, and poly(MPST)-grafted stainless steel substrates measured by XPS. The XPS spectrum of the original substrate showed carbon and oxygen signals in addition to metal signals. The carbon signal should be due to the

intrinsic carbon content of the steel alloy and/or the adsorption of trace amounts of hydrocarbon contaminants on the substrates. The strong O_{1s} signal in the original substrate should be due to hydrated oxides, which covered common metals and alloys under the ambient conditions. The presence of the hydrated oxides is favorable for the following silanization, because the coupling of a silane compound on a metal surface is believed to involve the following three steps [28, 29]: (1) hydrolysis of the silane coupling agents; (2) formation of hydrogen bonds; (3) formation of the metal-oxide bond (M-O-Si). After the silanization of the substrate, the corresponding silicone and sulfur signals were observed in the XPS spectrum with enhanced C_{1s} signal. The existence of metal signals indicates the formation of thin layer of the silane coupling agent on the substrate. After the graft polymerization of MPTS, the metal signals were not observed by XPS, suggesting the formation of thick layer of poly(MPTS).

Figure 2 shows ATR FT-IR spectra of the poly(MPTS) produced by solution polymerization under the same conditions as the graft polymerization, and the stainless-steel surface after the graft polymerization of MPTS. The spectrum of the poly(MPTS) was measured on the original stainless-steel substrate after dip coating in ethanol medium. It is worthy to point out that the original substrate did not show any peaks in the same range. In the case of the poly(MPTS) physically adsorbed on the original substrate, Si-O-C stretching vibration of the alkoxysilyl groups was observed at 1076cm^{-1}. On the other hand, in the case of the substrate after the graft polymerization of MPTS, the same spectrum as the poly(MPST) was observed. It is important to note that the spectrum of the poly(MPTS) physically adsorbed on the substrate was disappeared after washing with ethanol only one time, on the other hand, the poly(MPST) spectrum was observed on the grafted substrate after vigorous washing. From the above results, it was clear that the grafting of poly(MPTS) from the stainless steel surface was well conducted.

The HAp nanocrystals, which were calcined at 800°C, were coated on the

poly(MPTS)-grafted substrate through covalent bonding. Since the covalent bonding could not be observed directly on the substrate, the chemical bonding was estimated indirectly using the FT-IR analysis described in the previous article [7]. Figure 3 shows SEM photographs of the HAp-coated substrate after ultrasonic treatment. As a negative control, the original substrate, which was not modified with silane coupling agent and MPTS, was also used for the modification with the HAp nanocrystals. Although the HAp nanocrystals was adsorbed on the original substrate, they were almost removed by the ultrasonic treatment as shown in Fig. 3 (a). On the other hand, the crystals were remained on the poly(MPTS)-grafted surface, regardless of the morphology (spherical or rod-like) of the HAp crystals. The substrate was uniformly covered by the HAp nanocrystals without severe aggregations, because almost all nanocrystals could be dispersed in a medium by preventing the calcination-induced sintering among the crystals with the anti-sintering agent [24, 25].

Figures 4 shows SEM photographs of HUVEC morphologies on the sample substrates after 4 h of incubation. The cells seldom adhered on the original substrate for such a short period of incubation. On the other hand, the number of cells adhered on the HAp-coated substrates were much larger than that of the original substrate. This phenomenon can be explained because cell adhesion proteins such as fibronectin or vitronectin in a culture medium may be favorably adsorbed on the HAp surface [8]. In other words, it is clear that calcinated HAp coating on metallic substrates is effective way to obtain the affinity of cells.

Conclusion

A novel coating method of Type 316L stainless steel substrate with calcined HAp nanocrystals through covalent linkage was developed without high temperature treatment. The coating involved three steps: (1) silanization of the substrate for radical donation at 110°C; (2)